Structural and magnetic properties of $L1_0$-FePt nanoparticles aligned by external magnetic field

Yoshinori Tamada,[1,*] Shinpei Yamamoto,[2] Saburo Nasu,[1] and Teruo Ono[1]
[1]*Institute for Chemical Research, Kyoto University, Uji 611-0011, Japan*
[2]*Institute for Integrated Cell-Material Sciences, Kyoto University, Kyoto 606-8501, Japan*
(Received 4 September 2008; published 22 December 2008)

We investigated structural and magnetic properties of the easy-axis aligned $L1_0$-FePt nanoparticles by the combined use of x-ray diffraction (XRD), magnetization, and ^{57}Fe Mössbauer measurements. The $L1_0$-FePt nanoparticles were fixed in a polystyrene matrix by performing free radical polymerization of styrene under an aligning external magnetic field. Mössbauer spectrum of the $L1_0$-FePt nanoparticles/polystyrene composite showed tremendous decrease in the second and fifth absorption lines under the condition that the incident γ ray was parallel to the aligning field. This result indicates that the easy axes of the $L1_0$-FePt nanoparticles in the composite have a strong preferred orientation with a finite distribution. We estimated the distribution of easy-axis orientation by using the Mössbauer hyperfine parameters, which is in good agreement with that determined by the XRD rocking curve.

DOI: 10.1103/PhysRevB.78.214428 PACS number(s): 81.07.Bc, 33.45.+x

I. INTRODUCTION

Ferromagnetic FePt alloy with the ordered $L1_0$ structure is composed of alternatingly stacked layers of Fe and Pt atoms, and has the easy axis of the magnetization normal to the Fe and Pt layers (c axis). The FePt with the $L1_0$ structure possesses a large uniaxial crystal magnetic anisotropy energy (K_u, approximately 6×10^6 J/m^3), which is about an order of magnitude larger than that of the currently used CoCr-based alloys. Since the strong anisotropy can suppress superparamagnetic limit at the room temperature down to a particle size of about 3 nm, FePt nanoparticle is expected as one of promising candidates for the magnetic recording media with ultrahigh densities beyond 1 Tbit/in.^{2} in the near future.[1–5] The FePt nanoparticles synthesized by chemical solution based methods attract much attention from the viewpoint of practical use because of their well-defined morphology and easiness of handling for the fabrication of desirable arrays on substrates through being dispersible in solvents.[6–17] However, the chemical solution based methods can produce only disordered face-centered cubic (fcc) or partially ordered $L1_0$-FePt nanoparticles. The fcc-FePt nanoparticles are in the superparamagnetic state at room temperature owing to the low magnetic anisotropy. Although post-thermal annealing at high temperatures can transform the disordered fcc and the partially ordered $L1_0$ structure into the desired well-ordered $L1_0$ structure, it usually causes coalescence and coarsening of the nanoparticles giving rise to difficulties in fabricating desirable arrays on substrates. In addition, the post-thermal annealing also leads to difficulties in controlling the directions of the magnetic easy axes of the nanoparticles.

We have solved these problems by developing a synthetic strategy named "SiO_2-nanoreactor" method.[18–26] This synthetic method is characterized by the formation of SiO_2 layer on the surface of the precursory fcc-FePt nanoparticles that suppresses sintering of nanoparticles during the postannealing with keeping a single domain structure.[18–20] The studies using transmission electron microscopy (TEM), powder x-ray diffraction (XRD), superconducting quantum interference device (SQUID), and Mössbauer spectroscopy revealed that the $L1_0$-FePt nanoparticles synthesized by this method are free from aggregations and have a well-ordered $L1_0$ structure with single crystal. It is also worth noting that the $L1_0$-FePt nanoparticles can be made dispersible in various solvents with the aid of proper surfactants, and that the orientation of the magnetic easy axes of the solvent-dispersed nanoparticles can be controlled by the nanoparticle rotation with an external magnetic field.[18,19] By taking these advantages, we succeeded in preparing $L1_0$-FePt nanoparticles/polystyrene composites, in which the easy-axis aligned $L1_0$-FePt nanoparticles are dispersed and fixed.[25] Macroscopic characterizations such as SQUID magnetometry and XRD measurement revealed that the easy axes of the $L1_0$-FePt nanoparticles in the composite possess a strongly preferred orientation with a finite distribution. Our previous studies strongly indicate that the $L1_0$-FePt nanoparticles prepared by this method are suited for fabrication of arrays on substrates with their magnetic easy axes oriented normal to the surface. This is one of the key issues in realizing nanoparticle-based magnetic recording media.

In this paper, we report detailed studies on structural and magnetic properties of the easy-axis aligned $L1_0$-FePt nanoparticles with particular emphasis on analyses by means of ^{57}Fe Mössbauer spectroscopy. The ^{57}Fe Mössbauer spectroscopy is a sensitive tool for the investigation of the local electronic state of the Fe probe atoms. Such a microscopic characterization technique is of great importance especially for nanoparticles, which often exhibit different magnetic properties from bulk state due to the large surface to volume ratio. It is also worth noting that this measurement method enables us to estimate the direction of magnetic moments of Fe atoms and to obtain necessary parameters for determining distribution of the easy-axis direction of $L1_0$-FePt nanoparticles. It was found that the distribution estimated from the Mössbauer measurements was in good agreement with the results from the macroscopic characterization technique, i.e., the XRD rocking curve.

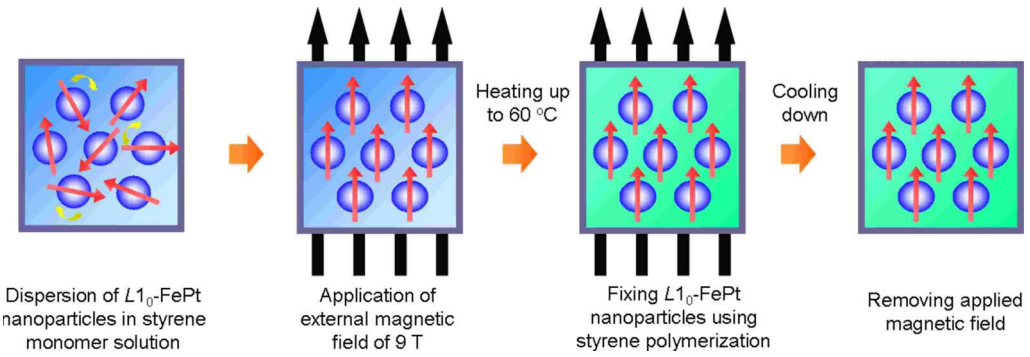

FIG. 1. (Color online) Schematic illustration of preparation of the $L1_0$-FePt nanoparticles/polystyrene composite under an external magnetic field.

II. EXPERIMENT

A. Preparation of the $L1_0$-FePt nanoparticles/polystyrene composite

The $L1_0$-FePt nanoparticles were prepared based on the SiO_2-nanoreactor method.[18–26] Precursory fcc-FePt nanoparticles were synthesized by basically the same way as in the initial work of Sun *et al.*,[6] and were subsequently coated by SiO_2 according to the method of Fan *et al.*[27] The elemental composition of the nanoparticles was determined to be $Fe_{51}Pt_{49}$. The SiO_2-coated fcc-FePt nanoparticles were then annealed at 900 °C for 1 h in a flowing $H_2(5\%)/Ar(95\%)$ gas for the transformation from fcc to the $L1_0$ structure. The $L1_0$-FePt nanoparticles dispersible in organic solvents were prepared by the aqueous/organic biphasic reaction.[20] In this reaction, the SiO_2 layer on the surface of the $L1_0$-FePt nanoparticles was dissolved off in aqueous sodium hydroxide solution, and thus-formed bare $L1_0$-FePt nanoparticles were extracted to the chloroform phase. The $L1_0$-FePt nanoparticles were collected by centrifugation after adding ethanol and were again dispersed in chloroform containing a small amount of oleic acid and oleyl amine.

The $L1_0$-FePt nanoparticles/polystyrene composite was prepared as follows: First, the $L1_0$-FePt nanoparticles dispersed in chloroform were collected by centrifugation after adding ethanol and were dispersed in styrene monomer solution with the FePt concentration of 3.2 wt %.[25,26] This solution also contained oleic acid (0.1 wt %), oleyl amine (0.1 wt %), and azobisisobutyronitrile (1 wt %). The azobisisobutyronitrile acts as an initiator of radical polymerization of styrene. Magnetic interactions between each $L1_0$-FePt nanoparticles are considered to be negligible because of the sufficiently low concentration of FePt nanoparticles. Then, the solution was kept at 60 °C for 18 h under argon atmosphere while applying an external magnetic field of 9 T. During this period, the free radical polymerization of styrene proceeds almost completely and thus-formed polystyrene matrix acts as a binder to fix the direction of easy axes of the $L1_0$-FePt nanoparticle, which are aligned parallel to the external magnetic field. These processes are schematically illustrated in Fig. 1. The obtained $L1_0$-FePt nanoparticles/polystyrene composite is shown in Fig. 2. The cylindrical composite has a diameter of 10 mm and a height of 12 mm. The magnetic aligning field was applied perpendicular to the top and bottom faces of the composite. Movement of the $L1_0$-FePt nanoparticles at room temperature was suppressed by glassy polystyrene matrix since the typical glass transition temperature of polystyrene is around 100 °C.[28] It is worth noting here that the particle orientation was found to be stable at room temperature at least for 1 year.

B. Characterization methods

TEM observations were performed using a JEOL JEM-1010D. TEM specimens were prepared by dissolving the composite in chloroform, a good solvent for polystyrene, and dropping the particle-containing solution on a carbon-coated copper grid. We scraped off a small piece of the composite and subsequently immersed it in chloroform under vigorous stirring. After stirring for 12 h, the $L1_0$-FePt nanoparticles were collected by centrifugation and were again dispersed in chloroform with the aid of a small amount of oleic acid and oleyl amine. The nanoparticle composition was determined by means of energy-dispersive x-ray analysis (EDX) on a JEOL JED 2140. For the EDX measurements, the nanoparticles dispersed in chloroform were precipitated by adding ethanol and then sufficiently dried. XRD profiles were collected on a Rigaku RINT2500 using Cu $K\alpha$ radiation. Magnetic properties were measured using a physical property measurement system (PPMS; Quantum Design) with an alternate current magnetization measurement system acces-

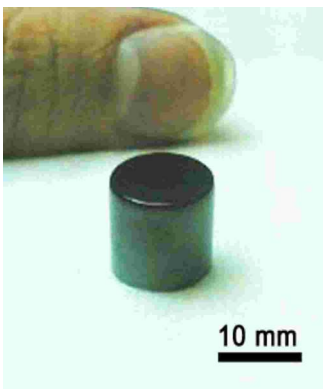

FIG. 2. (Color online) Photograph of the $L1_0$-FePt nanoparticles/polystyrene composite.

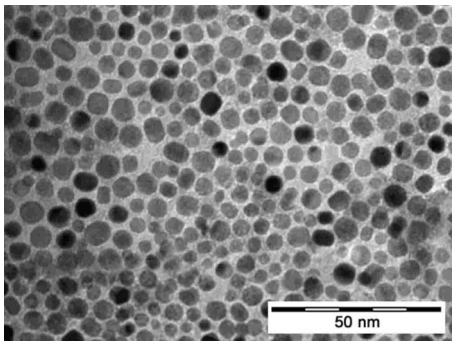

FIG. 3. TEM image of the $L1_0$-FePt nanoparticles in the composite. The specimens were prepared by dissolving the segment of the composite in chloroform.

sory. ^{57}Fe Mössbauer measurements were performed in transmission geometry using a radioactive source of ^{57}Co in Rh matrix with a constant acceleration mode. The Mössbauer hyperfine parameters of each spectrum observed were determined by the least square fit using a thin foil approximation. The velocity scale of spectra and the isomer shift value are relative to α-Fe at room temperature. All the values of isomer shift shown in this report are not corrected for the second-order Doppler shift.

III. RESULTS AND DISCUSSION

A. Macroscopic characterization of easy-axis aligned $L1_0$-FePt nanoparticles

Figure 3 shows a TEM image of the $L1_0$-FePt nanoparticles having been contained in the composite. The TEM image clearly shows that nanoparticles were well dispersed without aggregation even after the fixation process. Figure 4 shows size distribution of the $L1_0$-FePt nanoparticles. The average particle diameter and the standard deviation were estimated to be 5.1 and 1.2 nm, respectively.

Figure 5(a) shows XRD profile of the $L1_0$-FePt nanoparticles/polystyrene composite. The XRD measurement was performed under the condition that the top face of the cylindrical composite shown in Fig. 2 was set as the diffracting plane. This face was perpendicular to the direction of the aligning field. Powder XRD profile[29] of the

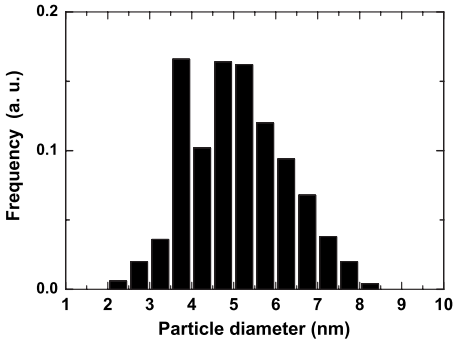

FIG. 4. Size distribution of the $L1_0$-FePt nanoparticles contained in the composite.

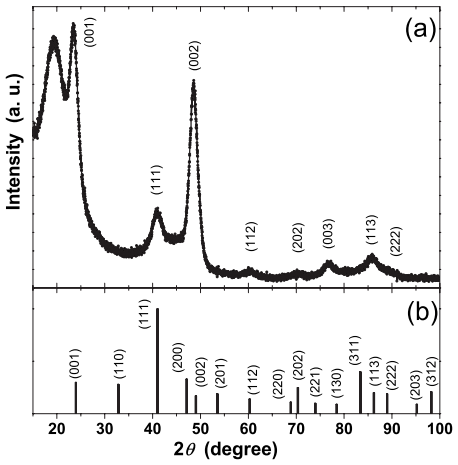

FIG. 5. XRD profiles of (a) the composite and (b) nonorientated powder pattern of $L1_0$-FePt alloy (Ref. 29).

$L1_0$-FePt alloy without preferred orientation was also shown in Fig. 5(b) for comparison. The broad peak around $2\theta = 22°$ in Fig. 5(a) comes from glassy polystyrene matrix. The XRD profile of the composite shows enhanced intensities of the (001) superlattice peak and the (002) fundamental peak in comparison with those of the reference profile with no preferred orientation. Moreover, the (003) superlattice peak which had been observed only in epitaxially grown $L1_0$-FePt thin films was also observed clearly, revealing that the easy axes of the $L1_0$-FePt nanoparticles in the composite possess a strong (001) preferred orientation.[30] However, the profile also shows other diffraction peaks such as (11l) peaks. Possible origins of the appearance of these peaks are as follows: one is the presence of a small amount of the fcc-FePt nanoparticles. Our previous works revealed that a small amount of fcc-FePt nanoparticles still remained unconverted to the $L1_0$ structure under the present annealing condition.[21–24] The fcc-FePt nanoparticles are randomly oriented in the composite since they are in the superparamagnetic state during the fixation process. Therefore, it is highly expected that the intensities of the (111), (200), (311), and (222) peaks are affected by presence of the fcc phase. The other is a finite distribution of the easy-axis direction of the $L1_0$-FePt nanoparticles. In the aligning process using an external magnetic field, it is well known that the direction of magnetization always fluctuates by thermal agitation. Furthermore, the fixation was performed at a relatively high temperature of 60 °C, resulting in a broader distribution of the easy-axis direction.

Figure 6 shows hysteresis loops of the composite measured at 300 K for applied fields perpendicular and parallel to the aligning field direction. Hereafter, we denote these measurement geometries as perpendicular and parallel geometries, respectively. Here, M_s is defined as the overall sample magnetization at −90 kOe measured under the parallel geometry. The shape of two hysteresis curves differs significantly, indicating that the composite has strong magnetic anisotropy. Coercivities observed in perpendicular and parallel geometries are 2.5 and 23 kOe, respectively. It is worth noting that successful measurement of the hysteresis curves implies that the nanoparticles in the composite are fixed

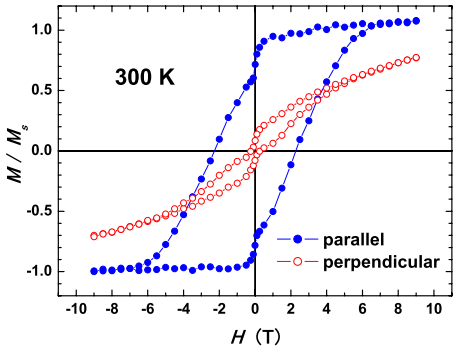

FIG. 6. (Color online) Hysteresis loops of the composite measured at 300 K for applied fields parallel and perpendicular to the aligning field direction.

strongly not to rotate even under the strong magnetic field of 90 kOe. The hysteresis loop measured under the parallel geometry possesses remanent magnetization almost equal to M_s, being consistent with the result of the XRD measurement which suggests that the easy axes of the $L1_0$-FePt nanoparticles are orientated parallel to the aligning field. However, squareness of the hysteresis loop is not so high, revealing that the nanoparticles in the composite have a certain distribution of reversal field. We consider that the distribution can be caused mainly by two reasons. One is the distribution of size of $L1_0$-FePt nanoparticles, which can be seen in the TEM image (Fig. 3). The other is distribution of easy-axis direction of $L1_0$-FePt nanoparticles fixed in the composite. Deviation of easy-axis direction of the nanoparticles from the aligning field direction can lower their coercivities. We note here that the kink observed at low magnetic field comes from a minor component of fcc-FePt nanoparticles mixed in the well-ordered $L1_0$ phase. The amount of the fcc-FePt nanoparticles, which is estimated from the decrease in magnetization at the kink of the hysteresis loop at 0 T, is about 20%. Since the fcc-FePt nanoparticles are in superparamagnetic state, we could remove the contribution of the fcc-FePt nanoparticles from the measured hysteresis loops. A rough estimate from the thus-obtained hysteresis loops of $L1_0$-FePt nanoparticles gives a value of K_u of 3.0×10^6 J/m^3, which is about half of the value reported in the bulk state.

B. Microscopic characterization of easy-axis aligned $L1_0$-FePt nanoparticles

To discuss the directions of magnetic moments and the microscopic magnetic properties of FePt nanoparticles in the composite, the ^{57}Fe Mössbauer measurements were performed at 300 K in transmission geometry in the absence of external magnetic field. The whole composite was used as a specimen for the measurements because of the low concentration of FePt nanoparticles. The Mössbauer spectra, which were measured under the conditions that the direction of incident γ ray was perpendicular and parallel to the aligning field, are shown in Figs. 7(a) and 7(b). Hereafter, we denote again these measurement geometries as perpendicular and parallel geometries. Full widths at half maximum (FWHMs)

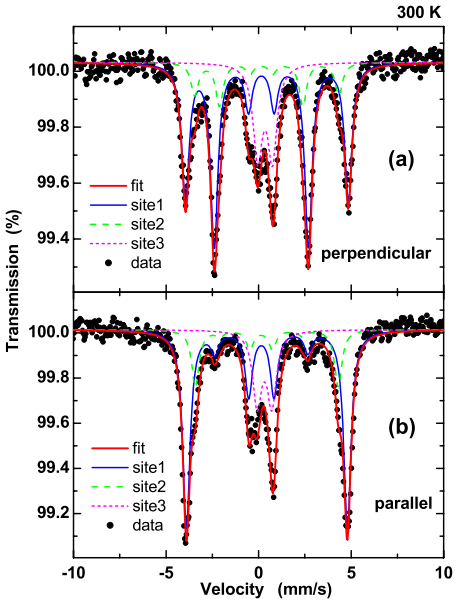

FIG. 7. (Color online) Mössbauer spectra of the composite measured at 300 K for applied field (a) perpendicular and (b) parallel to the aligning field. Site 1 (blue solid line), site 2 (green dashed line), and site 3 (purple dotted line) are attributed to core-$L1_0$-FePt, surface-$L1_0$-FePt, and fcc-FePt nanoparticles, respectively.

obtained from the least-squares-fitted lines of sites 1 and 2 shown in both figures [Figs. 7(a) and 7(b)] were assumed to be equal.

Figure 7(a) shows Mössbauer spectrum measured under the perpendicular geometry. It clearly shows the increase in the intensities of second and fifth absorption lines in comparison with those of the nonorientated $L1_0$-FePt nanoparticles, indicating that the easy axes of the $L1_0$-FePt nanoparticles in the composite have a strong preferred orientation. Relative intensity of the first and second absorption lines of the nonoriented sample is known to be 3/2, neglecting the thickness effect. Here, we define that ferromagnetic sextet absorption lines in Mössbauer spectrum are numbered from the left i.e., low velocity, one. The Mössbauer spectrum can be well fitted with three subspectra: core-$L1_0$-FePt (site 1), surface-$L1_0$-FePt (site 2), and fcc-FePt nanoparticles (site 3). The parameters of the subspectra are listed in Table I. The values of isomer shift (IS), hyperfine field (HF), quadrupole splitting (QS) of site 1 are in good agreement with those of the bulk $L1_0$-FePt alloy.[31,32] The α_g is a parameter for providing information on the orientation of the easy axes of the $L1_0$-FePt nanoparticles, and is defined by using relative intensity of the first and second absorption lines, as described later. The α_g value of site 1 is calculated to be 81.9°, indicating that almost all of the $L1_0$-FePt nanoparticles in the composite are aligned with the easy axes perpendicularly oriented to the direction of the incident γ ray. Site 2 also has the values of IS and QS being in good agreement with those of the bulk $L1_0$-FePt alloy, but the value of HF is slightly smaller than that of the bulk one. This tendency was also observed in previous works and is probably due to surface effects.[21,23] From the ratio of areal fraction (AREA) of site 1 to site 2, about 25% of Fe atoms in the $L1_0$-FePt nanoparticle

TABLE I. Mössbauer hyperfine parameters of easy-axis aligned $L1_0$-FePt nanoparticles measured under the condition that the direction of incident γ ray was perpendicular to that of the aligning field at 300 K.

	IS (mm/s)	HF (T)	QS (mm/s)	α_g (deg)	FWHM (mm/s)	AREA (%)
Site 1	0.30 ± 0.01	27.3 ± 0.8	0.30 ± 0.01	81.9 ± 2.5	0.45 ± 0.01	64.3 ± 3.2
Site 2	0.29 ± 0.01	23.9 ± 0.7	0.30 ± 0.01	81.9 ± 2.5	0.45 ± 0.01	15.3 ± 0.8
Site 3	0.35 ± 0.01	0	0.85 ± 0.03		0.65 ± 0.02	20.4 ± 1.0

are considered to locate on the surface, which is a reasonable value considering the size of the nanoparticle. The best fit of the Mössbauer spectrum was obtained under the condition that site 1 and site 2 have the same α_g value of 81.9°. It means that the magnetic moments of the Fe atoms on the surface point to the same direction as that of the core part of the nanoparticles. Other models such as magnetic moments of the surface Fe atoms point randomly and perpendicular to the surface of the nanoparticle resulted in limited success. The hyperfine parameters for site 3 are fixed to values determined from the independently measured spectrum of the superparamagnetic fcc-FePt nanoparticles. These parameters are in accord with reported ones, but the origin of large QS value was not understood completely at present.[33] Site 3 shows a paramagnetic doublet, indicating the fcc FePt nanoparticles at room temperature are superparamagnetic. Areal ratio of site 3 (approximately 20%) is in good agreement with the amount of magnetically soft phase (approximately 20%) estimated from the magnetization measurement at 300 K (Fig. 6).

Figure 7(b) shows Mössbauer spectrum measured under the parallel geometry. Tremendous decrease in the second and fifth absorption lines is clearly observed, again indicating that the easy axes of the $L1_0$-FePt nanoparticles in the composite possess a strong preferred orientation. The Mössbauer spectrum can be also well fitted with three subspectra: core-$L1_0$-FePt (site 1), surface-$L1_0$-FePt (site 2), and fcc-FePt nanoparticles (site 3). The parameters of the subspectra are listed in Table II. The values of IS, HF, QS, FWHM, and AREA of the all sites are almost the same as those obtained from the Mössbauer spectrum collected under the perpendicular geometry (Table I). It is a reasonable result because the hyperfine parameters except for α_g should be independent on direction of the incident γ ray. The α_g value of the site 1 was calculated to be 22.4°, which is substantially smaller than the value of random orientation of 54.7°. It is called the magic angle and means the random orientation of magnetic moments. The best fit of the Mössbauer spectrum was, again, obtained under the condition that site 1 and site 2 have the same α_g value (22.4°). It further supports the idea that the magnetic moments of the Fe atoms on the surface point to the same direction as that of the core.

C. Estimation of distribution of easy axis based on Mössbauer spectroscopy

The experimental results revealed that the easy axes of the $L1_0$-FePt nanoparticles in the composite have a strongly preferred orientation with a finite distribution. Since the presence of a finite distribution is inevitable in the magnetic field alignment process, the detailed and quantitative estimation of the distribution is very important. So as to quantitatively estimate distribution of the orientation, we used the α_g parameter of site 1 (22.4°) obtained under the parallel geometry.

In general, relative intensities of the nth absorption line (I_n) in ferromagnetic sextet are given as Eq. (1),[34,35]

$$I_{1,6}:I_{2,5}:I_{3,4} = \frac{3}{2}(1+\cos^2\alpha):2\sin^2\alpha:\frac{1}{2}(1+\cos^2\alpha). \quad (1)$$

Here, α is the angle between the direction of incident γ ray and that of magnetic moment of ^{57}Fe atom. We note again that the ferromagnetic sextet absorption lines in Mössbauer spectrum are numbered from the left, i.e., low velocity, one. The direction of easy axis of the nanoparticle can be considered to be parallel to that of magnetic moment of Fe atoms in the core of nanoparticle. Therefore, α is also the angle between the direction of incident γ ray and that of easy axis of the $L1_0$-FePt nanoparticle in the composite. In addition, we define the angle between the direction of aligning field and that of easy axis of the nanoparticle as ω. These geometries are summarized in Fig. 8.

In what follows, we estimate the distribution of orientation of the easy axis using a Mössbauer parameter α_g of 22.4° obtained under the parallel geometry. The α_g is given as Eq. (2) using the ratio of I_2 and I_1,

TABLE II. Mössbauer hyperfine parameters of easy-axis aligned $L1_0$-FePt nanoparticles measured under the condition that the direction of incident γ ray was parallel to that of the aligning field at 300 K.

	IS (mm/s)	HF (T)	QS (mm/s)	α_g (deg)	FWHM (mm/s)	AREA (%)
Site 1	0.30 ± 0.01	27.3 ± 0.8	0.30 ± 0.01	22.4 ± 0.7	0.45 ± 0.01	65.1 ± 3.3
Site 2	0.29 ± 0.01	23.9 ± 0.7	0.30 ± 0.01	22.4 ± 0.7	0.45 ± 0.01	15.5 ± 0.8
Site 3	0.35 ± 0.01	0	0.85 ± 0.03		0.65 ± 0.02	19.4 ± 1.0

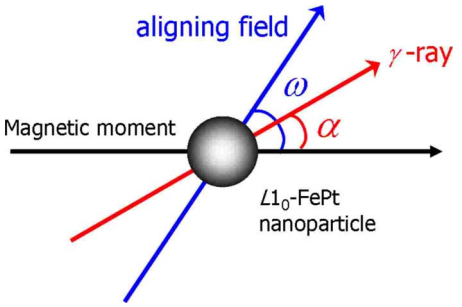

FIG. 8. (Color online) Definitions of α, the angle between the particle magnetization and incident γ ray, and ω, the angle between the particle magnetization and aligning field.

$$\frac{I_2}{I_1} = \frac{2\sin^2\alpha_g}{\frac{3}{2}(1+\cos^2\alpha_g)}. \tag{2}$$

It is well known that I_2/I_1 of nonoriented sample becomes 2/3. Equation (2) actually yields I_2/I_1 of 2/3 when α_g becomes the value of random orientation of 54.7°. In the present case, α_g of 22.4° gives I_2/I_1 ratio of 0.104. However, this calculation has a very limited meaning: I_2/I_1 ratio becomes 0.104 when all of the $L1_0$-FePt nanoparticles have α of 22.4°. However, such a situation never happens under the present experimental condition, and the presence of the distribution of easy axes should be taken into account. So we assumed that the distribution of easy-axis orientation of the $L1_0$-FePt nanoparticles in the composite obeyed normal (Gaussian) distribution $D(\alpha)$ with a mean of 0° and a standard deviation of σ. The $D(\alpha)$ is given as Eq. (3),

$$D(\alpha) = \frac{1}{\sqrt{2\pi}\sigma}\exp\left(\frac{-\alpha^2}{2\sigma^2}\right). \tag{3}$$

We estimated $D(\alpha)$ that can reproduce the I_2/I_1 ratio of 0.104.[35] So as to sum the contributions of all nanoparticles, the I_2/I_1 ratio was calculated using Eq. (4),

$$\frac{I_2}{I_1} = \frac{\int_0^{4\pi} 2\sin^2\alpha D(\alpha)d\Omega}{\int_0^{4\pi}\frac{3}{2}(1+\cos^2\alpha)D(\alpha)d\Omega} = \frac{\int_0^{\pi} 4\sin^3\alpha D(\alpha)d\alpha}{\int_0^{\pi} 3(2\sin\alpha-\sin^3\alpha)D(\alpha)d\alpha}. \tag{4}$$

Here, Ω is solid angle. From Eqs. (3) and (4), the I_2/I_1 ratio is a function of σ. We can see that if σ approaches infinity and 0, I_2/I_1 ratio approaches 2/3 and 0, respectively. These trends are consistent with the results from the Mössbauer measurement of randomly and highly orientated samples. Using I_2/I_1 ratio of 0.104, we could estimate value of σ to be 16.5°. Figure 9 shows $D(\alpha)$ with σ=16.5°. It was found that almost all of the nanoparticles have angles of less than 50°

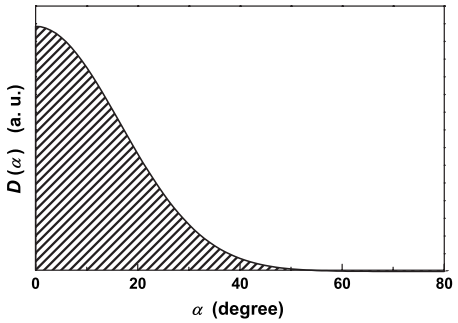

FIG. 9. Normal distribution curve with the standard deviation of 16.5°.

between their easy axis and the aligning field. It is noted that the aligning field is parallel to the incident γ ray under the present measurement geometry. Therefore, $D(\alpha)$ can also be considered as $D(\omega)$, which is the distribution of magnetic easy axes as a function of the deviation angle from the aligning field. If the nanoparticles having distribution of the easy axes of $D(\alpha)$ with σ=16.5° are exposed to the γ ray perpendicular to the aligning field, α_g is estimated to be 77.8°. This value is in good agreement with that (81.9°) obtained under the perpendicular geometry. It further supports the validity of the estimated distribution of $D(\alpha)$ with σ=16.5°.

So as to further confirm the validity of the estimated distribution, we performed the XRD rocking curve measurement, which gives information on distribution of easy-axis direction directly.[20,21] The rocking curve measurement was performed by using the (002) peak of the $L1_0$-FePt alloy. For this measurement, we cut the middle portion of the composite into a thin segment with 1 mm in thickness. The direction of cutting was set parallel to the aligning field. The measured rocking curve is shown in Fig. 10. It has a symmetrical shape with the maximum intensity at 0° and then decreases with increasing or decreasing θ. The intensity at certain θ directly represents the probability of finding a particle oriented at an angle of θ. We note here that θ is equal to the angle between the direction of aligning field and that of easy axis of the nanoparticle. Therefore, the rocking curve measurement directly gives $D(\omega)$. The distribution of easy-axis direction estimated from the Mössbauer and the rocking curve measurements are summarized in Fig. 11. They show good agreement with each other on average. It strongly indicates that the proper analysis enables us to estimate the distribu-

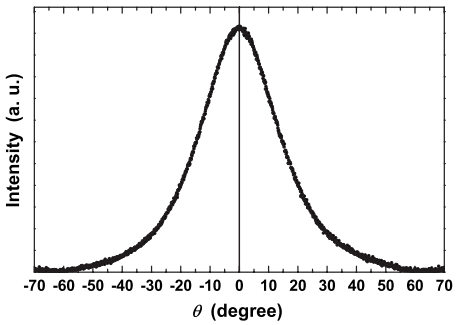

FIG. 10. Rocking curve of the composite measured by using (002) diffraction.

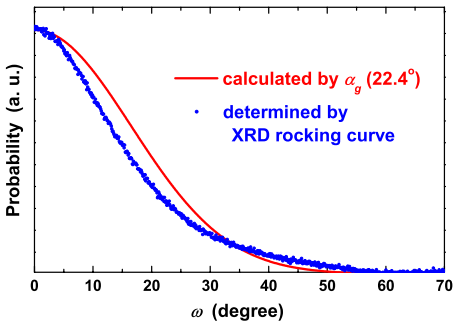

FIG. 11. (Color online) Distribution of easy-axis orientation estimated from the Mössbauer and the rocking curve measurements.

tion of direction of the magnetic easy axes, although Mössbauer spectroscopy only measures the average displacement of the easy axes from the instrument axis.

IV. CONCLUSION

In summary, we investigated structural and magnetic properties of the easy-axis aligned $L1_0$-FePt nanoparticles by XRD, magnetization, and ^{57}Fe Mössbauer measurements. Particular emphasis was placed on the ^{57}Fe Mössbauer measurements so as to investigate both microscopic magnetic and structural properties of the composite. It was revealed that the $L1_0$-FePt nanoparticles/polystyrene composite has a strong magnetic anisotropy arising from the strong preferred orientation of the easy axes of the $L1_0$-FePt nanoparticles in the composite. Mössbauer spectra of the composite measured under the condition that the incident γ ray parallel and perpendicular to the aligning field showed the decreased and increased intensity of the second and fifth absorption lines, respectively. In addition, the Mössbauer measurements suggested that the magnetic moments of Fe atoms on the surface point to the same direction as that of the core. We also tried to estimate the distribution of the magnetic easy axes by analyzing the Mössbauer hyperfine parameter. By assuming that the distribution obeys normal distribution, we estimated the standard deviation to be 16.5°. This result means that almost all of the nanoparticles have angles of less than 50° between their easy axis and the aligning field. This estimated distribution showed good agreement with that determined by the XRD rocking curve measurement. Since one of the key issues for the realization of $L1_0$-FePt nanoparticle-based recording media is formation and fixation of an array on a substrate with the magnetic easy-axis oriented substrate normal, these conclusions could open a way to prepare the prototype of the magnetic recording media using $L1_0$-FePt nanoparticles.

ACKNOWLEDGMENTS

The authors express their thanks to the Ministry of Education, Culture, Sports, Science and Technology of Japan (MEXT, Japan) Grant-in-Aid for Creative Scientific Research and Global Center of Excellence (GCOE). Y.T. thanks the support by Japan Society for the Promotion of Science (JSPS) Research Foundation for Young Scientists and by Support Center for Advanced Telecommunications Technology Research, Foundation (SCAT).

*tama@ssc1.kuicr.kyoto-u.ac.jp

[1] K. Inomata, T. Sawa, and S. Hashimoto, J. Appl. Phys. **64**, 2537 (1988).
[2] T. Klemmer, D. Hoydick, H. Okumura, B. Zhang, and W. A. Soffa, Scr. Metall. Mater. **33**, 1793 (1995).
[3] D. Weller, A. Moser, L. Folks, M. E. Best, W. Le, M. F. Toney, M. Schwickert, J. U. Thiele, and M. F. Doerner, IEEE Trans. Magn. **36**, 10 (2000).
[4] S. Shouheng, E. E. Fullerton, D. Weller, and C. B. Murray, IEEE Trans. Magn. **37**, 1239 (2001).
[5] S. Sun, Adv. Mater. (Weinheim, Ger.) **18**, 393 (2006).
[6] S. Sun, C. B. Murray, D. Weller, L. Folks, and A. Moser, Science **287**, 1989 (2000).
[7] J. W. Harrell, S. Wang, D. E. Nikles, and M. Chen, Appl. Phys. Lett. **79**, 4393 (2001).
[8] K. E. Elkins, T. S. Vendantam, J. P. Liu, H. Zeng, S. Sun, Y. Ding, and Z. L. Wang, Nano Lett. **3**, 1647 (2003).
[9] B. Jeyadevan, K. Urakawa, A. Hobo, N. Chinnasamy, K. Shinoda, K. Tohji, D. D. J. Djayaprawira, M. Tsunoda, and M. Takahashi, Jpn. J. Appl. Phys., Part 2 **42**, L350 (2003).
[10] S. Momose, H. Kodama, N. Ihara, T. Uzumaki, and A. Tanaka, Jpn. J. Appl. Phys., Part 2 **42**, L1252 (2003).
[11] Y. K. Takahashi, T. Koyama, M. Ohnuma, T. Ohkubo, and K. Hono, J. Appl. Phys. **95**, 2690 (2004).
[12] M. Chen, J. P. Liu, and S. Sun, J. Am. Chem. Soc. **126**, 8394 (2004).
[13] C. Liu, X. Wu, T. Klemmer, N. Shukula, X. Yang, D. Weller, A. G. Roy, M. Tanase, and D. Laughlin, J. Phys. Chem. B **108**, 6121 (2004).
[14] E. E. Carpenter, J. A. Sims, J. A. Wienmann, W. L. Zhou, and C. J. O'Connor, J. Appl. Phys. **87**, 5615 (2000).
[15] M. Nakaya, Y. Tsuchiya, K. Ito, Y. Oumi, T. Sano, and T. Teranishi, Chem. Lett. **33**, 130 (2004).
[16] S. Kang, J. W. Harrel, and D. E. Nikles, Nano Lett. **2**, 1033 (2002).
[17] E. V. Shevchenko, D. V. Talapin, H. Schnablegger, A. Kornowski, Ö. Festin, P. Svedlindh, M. Haase, and H. Weller, J. Am. Chem. Soc. **125**, 9090 (2003).
[18] S. Yamamoto, Y. Morimoto, T. Ono, and M. Takano, Appl. Phys. Lett. **87**, 032503 (2005).
[19] Y. Morimoto, T. Tamada, S. Yamamoto, T. Ono, and M. Takano, J. Magn. Soc. Jpn. **30**, 464 (2006).
[20] S. Yamamoto, Y. Morimoto, Y. Tamada, Y. K. Takahashi, K. Hono, T. Ono, and M. Takano, Chem. Mater. **18**, 5385 (2006).
[21] Y. Tamada, Y. Morimoto, S. Yamamoto, N. Hayashi, M. Takano, S. Nasu, and T. Ono, Jpn. J. Appl. Phys., Part 2 **45**, L1232 (2006).
[22] Y. Tamada, Y. Morimoto, S. Yamamoto, M. Takano, S. Nasu, and

T. Ono, J. Magn. Magn. Mater. **310**, 2381 (2007).
[23] Y. Tamada, S. Yamamoto, M. Takano, S. Nasu, and T. Ono, Appl. Phys. Lett. **90**, 162509 (2007).
[24] Y. Tamada, S. Yamamoto, M. Takano, S. Nasu, and T. Ono, Phys. Status Solidi C **4**, 4503 (2007).
[25] S. Yamamoto, Y. Tamada, T. Ono, and M. Takano, J. Magn. Soc. Jpn. **31**, 199 (2007).
[26] S. Yamamoto, Y. Tamada, K. Kobayashi, T. Ono, and M. Takano, J. Magn. Soc. Jpn. **32**, 66 (2008).
[27] H. Fan, K. Yang, D. M. Boye, T. Sigmon, K. J. Malloy, H. Xu, G. P. López, and C. J. Brinker, Science **304**, 567 (2004).
[28] *Polymer Handbook*, edited by J. Brandrup and E. H. Imergut (Wiley, New York, 1989).
[29] JCPDS Report No. 431359 (unpublished).
[30] T. Shima, K. Takanashi, Y. K. Takahashi, and K. Hono, Appl. Phys. Lett. **85**, 2571 (2004).
[31] T. Goto, H. Utsugi, and K. Watanabe, Hyperfine Interact. **54**, 539 (1990).
[32] T. Goto, H. Utsugi, and K. Watanabe, J. Alloys Compd. **204**, 173 (1994).
[33] B. Stahl, J. Ellrich, R. Theissmann, M. Ghafari, S. Bhattacharya, H. Hahn, N. S. Gajbhiye, D. Kramer, R. N. Viswanath, J. Weissmüller, and H. Gleiter, Phys. Rev. B **67**, 014422 (2003).
[34] E. Fujita, S. Nasu, T. Nishida, and Y. Yoshida, *Handbook on Mössbauer Spectroscopy* (Agune Technical Center, Tokyo, 1999).
[35] U. Gonser and H. D. Pfannes, J. Phys. (Paris) **35**, C6 (1974).